Progress In Electromagnetics Research B, Vol. 7, 105–115, 2008

COMPACT BANDPASS FILTERS UTILIZING DIELECTRIC FILLED WAVEGUIDES

H. Ghorbaninejad and M. Khalaj-Amirhosseini

College of Electrical Engineering
Iran University of Science and Technology
Tehran, Iran

Abstract—In this paper, a compact waveguide bandpass filter is proposed. The proposed structure consists of some inductive diaphragms in a rectangular waveguide and the regions between them have been filled fully by dielectrics. The relations between the physical and electrical parameters of the existed asymmetrical impedance invertors are obtained. The usefulness of the proposed structure and its performance are verified by designing and simulating an equal-ripple X-band bandpass filter.

1. INTRODUCTION

Waveguide bandpass filters are one of the inevitable requirements of microwave circuits. The straightforward approach to construct these filters is using inductive elements such as irises, rods, diaphragms and posts as impedance invertors between transmission line resonators, which are realized with half wavelength hollow waveguides [1–4]. Although some other approaches such as using waveguides filled by multi-layer dielectrics [5] and substrate integrated waveguides (SIWs) [6] have been introduced as bandpass filters by now. The long length of waveguide bandpass filters, which is due to hollow waveguide resonators, is a deficiency for them. In this paper, we propose to fill the region between two diaphragms fully by dielectrics to reduce the length of resulted filter. Asymmetrical impedance invertors appear in the proposed structure and we have to obtain the relations between their physical and electrical parameters. The usefulness of the proposed structure and its performance are verified by a comprehensive example and using HFSS software.

2. DIELECTRIC FILLED WAVEGUIDE FILTER

Figure 1 shows the proposed waveguide bandpass filter consisting of $N+1$ diaphragms and N dielectric filled regions in a rectangular waveguide. The cross section of the waveguide has dimensions of a and b. The n-th region ($n = 1, 2, \dots, N$) has been fully filled by a dielectric with relative electric permittivity ε_{rn}, where $\varepsilon_{r0} = \varepsilon_{r,N+1} = 1$. The characteristic impedance and the phase constant of the n-th dielectric filled region are as the followings, respectively.

$$Z_n = \frac{\eta_0}{\sqrt{\varepsilon_{rn} - (f_c/f)^2}} \tag{1}$$

$$\beta_n = \frac{\omega}{c}\sqrt{\varepsilon_{rn} - (f_c/f)^2} \tag{2}$$

where η_0 and c are the wave impedance and the velocity of the wave, respectively, in the free space. Also, f_c is the cutoff frequency of the hollow waveguide. The diaphragms, which act as shunt inductances, have an aperture of width g_n, whose values are determined in the next section. On the other hand, Fig. 2 shows a bandpass filter consisting of N series resonators and $N+1$ impedance invertors. The value of impedance invertors and the elements of resonators can be obtained

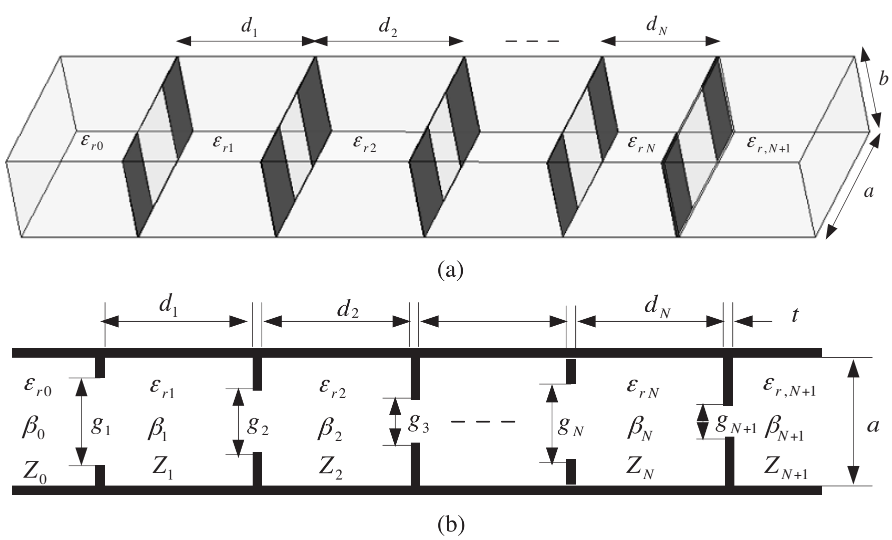

Figure 1. The proposed dielectric filled waveguide bandpass filter. (a) Three dimensional view. (b) Top view.

according to the type of filter transfer function, center frequency and the bandwidth of the filter [1–4].

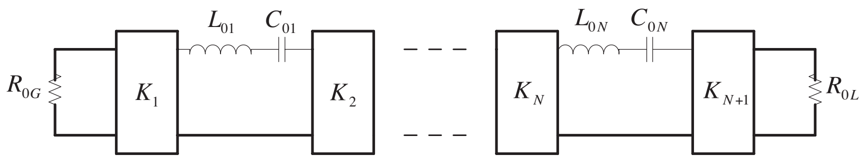

Figure 2. Typical bandpass filter using series resonators and impedance invertors.

Now, we want to model the proposed waveguide filter shown in Fig. 1 as a bandpass filter shown in Fig. 2. For this purpose, two following modelings are required:

1. Modeling series resonators by transmission lines of length half wavelength. Equating the $ABCD$ matrix and its derivative of a half wavelength waveguide transmission line with those of a series lumped resonators gives us the characteristic impedance of the n-th region as follows

$$Z_n = 4f_0 L_{0n} \frac{\varepsilon_r - (f_c/f_0)^2}{\varepsilon_r} \tag{3}$$

2. Modeling the impedance invertors by shunt inductances located between two transmission lines of negative length as shown in Fig. 3.

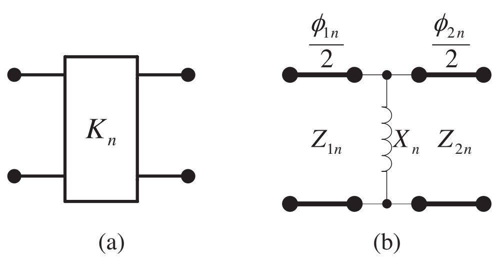

Figure 3. (a) An impedance invertor. (b) A circuit model for impedance invertors.

Using the above modelings, the circuit shown in Fig. 4 is determined, in which

$$D_n = \lambda_{gn}/2 = \frac{\pi}{\beta_n} = \frac{\lambda_0}{2\sqrt{\varepsilon_{rn} - (f_c/f_0)^2}} \tag{4}$$

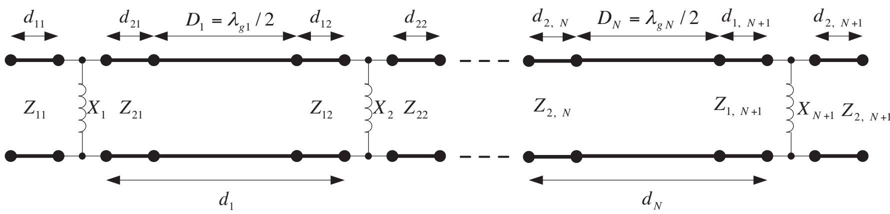

Figure 4. Transmission line realization of a dielectric filled waveguide bandpass filter.

where λ_0 is the wavelength of the free space at center frequency. Also, comparing Figs. 2 and 4 with each other results the following relations for $n = 1, 2, \dots, N$.

$$d_n = d_{2,n} + D_n + d_{1,n+1} \tag{5}$$

$$Z_{2,n} = Z_{1,n+1} = Z_n \tag{6}$$

$$\beta_{2,n} = \beta_{1,n+1} = \beta_n \tag{7}$$

$$Z_{2,N+1} = Z_{N+1} = R_{0G} = R_{0L} = Z_0 \tag{8}$$

Furthermore, according to Figs. 3 and 4, the lengths d_{1n} and d_{2n}, which are negative, are obtained from the following relations for $n = 1, 2, \dots, N+1$.

$$d_{1n} = \frac{1}{2}\frac{\phi_{1n}}{\beta_{1n}} \tag{9}$$

$$d_{2n} = \frac{1}{2}\frac{\phi_{2n}}{\beta_{2n}} \tag{10}$$

3. IMPEDANCE INVERTORS

The values of parameters of the circuit shown in Fig. 3(b) are known in the literature if $Z_{1n} = Z_{2n}$ (shunt inductance between two identical transmission lines). However, this equality is not existed in Fig. 4 especially at two ended impedance invertors (shunt inductance between two different transmission lines). So, we have to obtain the parameters of general model shown in Fig. 3, by equating the $ABCD$ matrices of two circuits with each other as follows

$$\begin{bmatrix} \cos(\phi_{1n}/2) & jZ_{1n}\sin(\phi_{1n}/2) \\ j/Z_{1n}\sin(\phi_{1n}/2) & \cos(\phi_{1n}/2) \end{bmatrix} \begin{bmatrix} 1 & 0 \\ -j/X_n & 1 \end{bmatrix} \begin{bmatrix} \cos(\phi_{2n}/2) & jZ_{2n}\sin(\phi_{2n}/2) \\ j/Z_{2n}\sin(\phi_{2n}/2) & \cos(\phi_{2n}/2) \end{bmatrix}$$
$$= \begin{bmatrix} 0 & jK_n \\ j/K_n & 0 \end{bmatrix} \tag{11}$$

After some mathematical manipulations one can obtained three following relations

$$\tan\left(\frac{\phi_{1n}+\phi_{2n}}{2}\right) = -\frac{(Z_{1n}+Z_{2n})\,X_n}{Z_{1n}Z_{2n}} \tag{12}$$

$$\tan\left(\frac{\phi_{1n}-\phi_{2n}}{2}\right) = \frac{(Z_{1n}-Z_{2n})\,X_n}{Z_{1n}Z_{2n}} \tag{13}$$

$$X_n = \frac{4K_n}{\sqrt{K_n^4(p_n-q_n)^2-8K_n^2(p_n+q_n)+16}} \tag{14}$$

where p_n and q_n are real values defined as follows

$$p_n = \frac{(Z_{1n}+Z_{2n})^2}{Z_{1n}^2 Z_{2n}^2} \tag{15}$$

$$q_n = \frac{(Z_{1n}-Z_{2n})^2}{Z_{1n}^2 Z_{2n}^2} \tag{16}$$

The formulas (12) and (13) can be arranged as the followings

$$\phi_{1n} = \tan^{-1}\left(\frac{(Z_{1n}-Z_{2n})X_n}{Z_{1n}Z_{2n}}\right)-\tan^{-1}\left(\frac{(Z_{1n}+Z_{2n})X_n}{Z_{1n}Z_{2n}}\right)<0 \tag{17}$$

$$\phi_{2n} = \tan^{-1}\left(\frac{(Z_{2n}-Z_{1n})X_n}{Z_{1n}Z_{2n}}\right)-\tan^{-1}\left(\frac{(Z_{1n}+Z_{2n})X_n}{Z_{1n}Z_{2n}}\right)<0 \tag{18}$$

4. THE INDUCTIVE DIAPHRAGMS

One of diaphragms existed in Fig. 1 and its equivalent circuit (shunt inductance) are shown in Figs. 5 and 6, respectively. The value of shunt

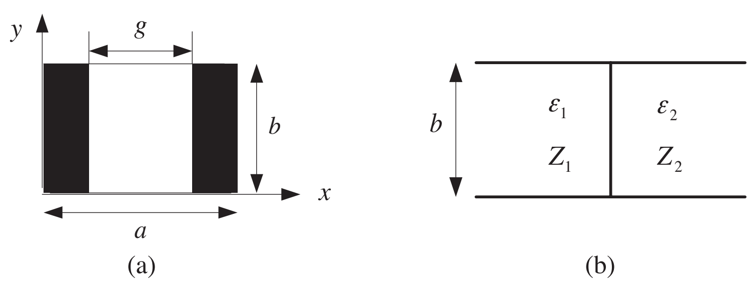

Figure 5. (a) The cross sectional view of a diaphragm. (b) The side view of a diaphragm.

inductance of this diaphragm is known in the literature if $Z_1 = Z_2$ (diaphragm between two identical mediums). However, this equality is not existed in Fig. 1 especially at two ended diaphragms (diaphragm between two different mediums). So, we have to obtain the value of shunt inductance of the circuit shown in Fig. 6.

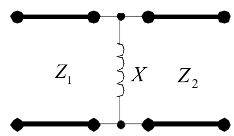

Figure 6. The equivalent circuit of a diaphragm.

It is assumed that only dominant mode TE_{10} can be propagated non-evanescently in the waveguide, i.e., $2a/3 < \lambda_0 < 2a$. The incident field TE_{10} will set up reflected and transmitted higher order modes. So we can write the transverse electric and magnetic fields as follows

$$E_y = \begin{cases} (e^{-j\beta_1 z} + Re^{j\beta_1 z})\sin(\pi x/a) + \sum_{m=2}^{\infty} R_m e^{\gamma_{1m} z}\sin(m\pi x/a) & z < 0 \\ Te^{-j\beta_2 z}\sin(\pi x/a) + \sum_{m=2}^{\infty} T_m e^{-\gamma_{2m} z}\sin(m\pi x/a) & z > 0 \end{cases} \tag{19}$$

$$H_x = \begin{cases} \frac{\beta_1}{\omega\mu}(e^{-j\beta_1 z} - Re^{j\beta_1 z})\sin(\pi x/a) \\ +\frac{j}{\omega\mu}\sum_{m=2}^{\infty}\gamma_{1m} R_m e^{\gamma_{1m} z}\sin(m\pi x/a) & z < 0 \\ \frac{\beta_2}{\omega\mu} Te^{-j\beta_2 z}\sin(\pi x/a) \\ -\frac{j}{\omega\mu}\sum_{m=2}^{\infty}\gamma_{2m} T_m e^{-\gamma_{2m} z}\sin(m\pi x/a) & z > 0 \end{cases} \tag{20}$$

where

$$\gamma_{1m} = \frac{\omega}{c}\sqrt{(mf_c/f)^2 - \varepsilon_{r1}} \tag{21}$$

$$\gamma_{2m} = \frac{\omega}{c}\sqrt{(mf_c/f)^2 - \varepsilon_{r2}} \tag{22}$$

The transverse electric field E_y on the diaphragm must be continuous on the aperture and must be zero out of the aperture.

Assuming $E_y(x, y, 0) = f(x)$ on the aperture and using Fourier analysis, we can obtain the following relations

$$1 + R = T = \frac{2}{a} \int_{(a-g)/2}^{(a+g)/2} f(x) \sin(\pi x/a) dx \tag{23}$$

$$R_m = T_m = \frac{2}{a} \int_{(a-g)/2}^{(a+g)/2} f(x) \sin(m\pi x/a) dx \quad \text{for } m = 2,\ 3, \ldots \tag{24}$$

Moreover, the transverse magnetic field H_x must be continuous on the aperture that gives the following relation

$$\begin{aligned} &-j\beta_1(1 - R) \sin(\pi x/a) + \sum_{m=2}^{\infty} R_m \gamma_{1m} \sin(m\pi x/a) = \\ &-j\beta_2 T \sin(\pi x/a) - \sum_{m=2}^{\infty} T_m \gamma_{2m} \sin(m\pi x/a) \end{aligned} \tag{25}$$

Using (23) and (24) in (25), we obtain the following relation gives us the following relation

$$\begin{aligned} &\left(\frac{\beta_1 + \beta_2}{\beta_1} - \frac{2}{T}\right) \sin(\pi x/a) \int_{(a-g)/2}^{(a+g)/2} f(x') \sin(\pi x'/a) dx' = \\ &j \sum_{m=2}^{\infty} \left[\left(\frac{\gamma_{1m} + \gamma_{2m}}{\beta_1}\right) \sin(m\pi x/a) \int_{(a-g)/2}^{(a+g)/2} f(x') \sin(m\pi x'/a) dx' \right] \end{aligned} \tag{26}$$

where x is over the diaphragm aperture. It is known that the normalized susceptance $\bar{B} = BZ_1 = -Z_1/X = B/Y_1$ causes a reflection R given by

$$\frac{2R}{1 + R} = 1 - j\bar{B} - \frac{Z_1}{Z_2} \tag{27}$$

According to (23) and (27), (26) turns to the following

$$\begin{aligned} &\bar{B} \sin(\pi x/a) \int_{(a-g)/2}^{(a+g)/2} f(x') \sin(\pi x'/a) dx = \\ &-\sum_{m=2}^{\infty} \left[\left(\frac{\gamma_{1m} + \gamma_{2m}}{\beta_1}\right) \sin(m\pi x/a) \int_{(a-g)/2}^{(a+g)/2} f(x') \sin(m\pi x'/a) dx' \right] \end{aligned} \tag{28}$$

Using an analytical method identical to the approach introduced in [7], in which only two evanescent modes have been considered, the following relation is obtained for the susceptance of the diaphragm shown in Fig. 5.

$$\bar{B} = -\frac{\lambda_g}{a}\left\{\frac{1}{s^2} - 1 - \frac{(1-s^2)^2}{1-\delta_3 s^6}\left[3\delta_3 + 5\delta_5 \frac{\left[2s^2 - 1 + \delta_3 s^6(s^2-2)\right]^2}{(1-\delta_3 s^6)(1-\delta_5 s^{10}) - 15 s^6 (1-s^2)^2 \delta_5}\right]\right\} \tag{29}$$

where $s = \sin(\pi g/2a)$ and $\delta_m = (\delta_{1m} + \delta_{2m})/2$, in which $\delta_{1m} = 1 - \sqrt{1 - \varepsilon_{r1}(f/mf_c)^2}$ and $\delta_{2m} = 1 - \sqrt{1 - \varepsilon_{r2}(f/mf_c)^2}$.

5. EXAMPLE AND RESULTS

In this section a compact bandpass filter is designed utilizing a WR-90 waveguide ($a = 0.9$ inches and $b = 0.4$ inches). We would like to design a 3-order chebyshev type bandpass filter with center frequency 10 GHz, the relative bandwidth 9 percent and equal ripples 0.5 dB. It is assumed that all three transmission line resonators have the same relative electric permittivity $\varepsilon_{r1} = \varepsilon_{r2} = \varepsilon_{r3} = 3.5$ (dielectric-filled filter) or $\varepsilon_{r1} = \varepsilon_{r2} = \varepsilon_{r3} = 1.0$ (air-filled filter). Using the relevant relations, the physical parameters of both filters are calculated as shown in Tables 1 and 2. After calculating these values, we should optimize them to have a better frequency response with attention to the effects of some factors such as the thickness of diaphragms and the coupling between contiguous diaphragms. The simulation and optimization of the filters are done using full-wave software HFSS, which is based on the finite element method (FEM) [8]. Simulation results of both air-filled and dielectric-filled structures are plotted in Figs. 7 and 8. It is seen that the performance of the dielectric-filled filter is identical to that of the air-filled filter while the length of former one is 21.57 mm and that of the latter one is 50.79 mm. Therefore, the dielectric-filled filter has more than 57% compactness compared to the conventional air-filled filter. From the above example one may satisfy about the good performance and compactness of dielectric-filled waveguide bandpass filter. Moreover, it is obvious that the advantages of the proposed filter could be mentioned as the followings:

1. It has a significant compactness compared to the conventional air-filled waveguide filters.
2. The fabrication is easy because the metals of diaphragms could

Table 1. The physical parameters of designed air-filled waveguide bandpass filter.

Lengths and Widths [mm]	d_1	d_2	d_3	g_1	g_2	g_3	g_4
Before Optimization	16.3161	17.5183	16.3161	5.1361	3.6877	3.6877	5.1361
After Optimization	16.5340	17.7212	16.5340	5.2361	3.7479	3.7479	5.2361

Table 2. The physical parameters of designed dielectric-filled waveguide bandpass filter.

Lengths and Widths [mm]	d_1	d_2	d_3	g_1	g_2	g_3	g_4
Before Optimization	6.8763	7.8969	6.8763	3.7196	1.9574	1.9574	3.7196
After Optimization	6.7987	7.9529	6.7987	3.9386	1.9750	1.9750	3.9386

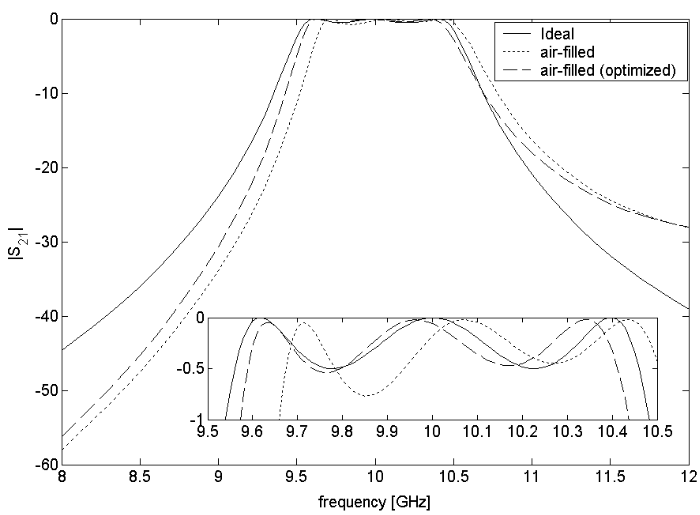

Figure 7. The simulation results of designed air-filled waveguide bandpass filter.

glue to the dielectrics and consequently the waveguide could be made monolithic instead of multi-sectional.

3. The mechanical stability is good because the diaphragms lean to the dielectrics.
4. It is suitable for high power microwave circuits because the breakdown voltage of dielectrics is higher than that of the air.

Of course, the above superiorities are in front of the losses of dielectrics and so we have to use low loss dielectrics.

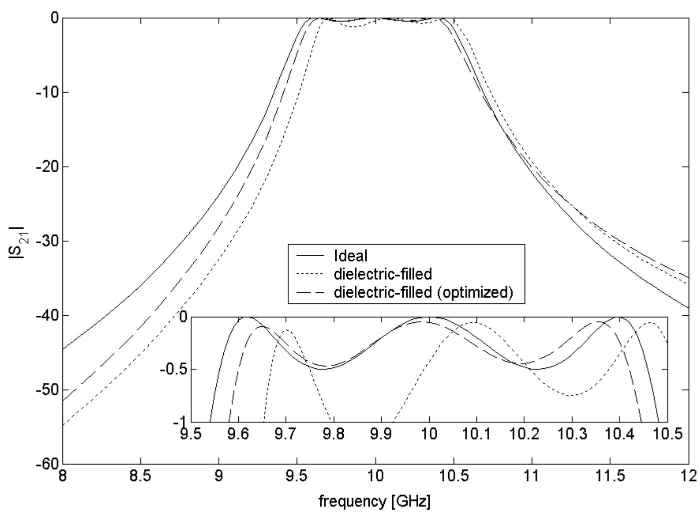

Figure 8. The simulation results of designed dielectric-filled waveguide bandpass filter.

6. CONCLUSION

A compact waveguide bandpass filter was proposed. The proposed structure consists of $N + 1$ inductive diaphragms in a rectangular waveguide and the regions between them have been filled fully by dielectrics. The relations between the physical and electrical parameters of the existed asymmetrical impedance invertors were obtained. The usefulness of the proposed structure and its performance are verified by designing and simulating an equal-ripple X-band bandpass filter. The designed filter has 57% compactness compared to the conventional filters. Moreover, the proposed filter has the advantages of easy fabrication, mechanical stability and capability of using in high power applications.

REFERENCES

1. Matthaei, G. L., L. Young, and E. M. T. Jones, "*Microwave Filters, Impedance-Matching Networks and Coupling Structures*, Artech House, Dedham, Mass., 1980.
2. Pozar, D. M., *Microwave Engineering*, Addison-Wesley, 1990.
3. Collin, R. E., *Foundations for Microwave Engineering*, McGraw-Hill, New York, 1996.
4. Levy, R., R. V. Snyder, and G. Matthaei, "Design of microwave filters," *IEEE Trans. Microwave Theory Tech.*, Vol. 50, 783–793, 2002.
5. Khalaj-Amirhosseini, M., "Microwave filters using waveguides filled by multi-layer dielectric," *Progress In Electromagnetics Research*, PIER 66, 105–110, 2006.
6. Sotoodeh, Z., B. Beglarbegian, F. H. Kashani, and H. Ameri, "A novel bandpass waveguide filter structure on SIW technology," *Progress In Electromagnetics Research Letters*, Vol. 2, 141–148, 2008.
7. Lewin, L., *Theory of Waveguides*, Butterworth & Co, Ltd., 1975.
8. HFSS Release 9.0, Ansoft Corp., 2003.